

Optimization of Wireless Power Transmission Systems with Parasitic Wires

K. H. Yeap, A. R. C. Cheah, K. Hirasawa, K. C. Yeong, K. C. Lai, and H. Nisar

Universiti Tunku Abdul Rahman, Kampar, Perak 31900, Malaysia
 yeapkh@utar.edu.my, agnescheah_91@hotmail.com, hirasawa@ieee.org, yeongkc@utar.edu.my,
 laikc@utar.edu.my, humaira@utar.edu.my

Abstract — We present a rigorous optimization method to design wireless power transmission (WPT) systems. In order to optimize the power coupled to the receiver, reactive parasitic components are integrated into the system. Simulated annealing is implemented in conjunction with the method of moments to determine the optimum parameters for the design. By carefully adjusting the geometry, size, position and properties of the parasitic wires, it could be seen that the peak efficiency and effective distance for power coupling could be significantly improved. The result shows that the implementation of a square parasitic wire gives better performance than a circular one. A WPT system with a square reactive wire gives respectively a 0.79% and 0.07 λ improvement in peak efficiency and effective distance compared to its zero-impedance counterpart. By inserting two square reactive wires with the transmitter sandwiched in between, the peak efficiency and effective distance are found to have increased respectively by 3.37% and 0.18 λ , compared to that with a single reactive wire.

Index Terms — Antennas, method of moments, simulated annealing, wireless power transmission.

I. INTRODUCTION

Throughout years of research and development, workable wireless power transmission (WPT) systems have already been made available [1]. However, there are still open issues and challenges yet to be overcome. According to the findings by Kurs et al. [2], the power efficiency of a WPT system operating at 9.9 MHz deteriorates below 50% at a distance greater than 2 m. It is apparent that the power transmission efficiency of a WPT system is constrained by the distance the power can be effectively transferred to the receiver. As a result of this, existing WPT devices can only operate at very close proximity. The rapid attenuation of the propagating energy is clearly one of the critical issues which require an immediate and effective solution.

The installation of parasitic elements into a wireless communication system is found to have significantly reduced signal attenuation and increase signal quality. In [3], a comparison was made between the performance of

a conventional Yagi-Uda transmitting antenna and that with parasitic elements constructed around it. It is found that the system installed with parasitic elements outperformed the conventional Yagi-Uda system -- the signal to interference noise ratio (SINR) and the voltage standing wave ratio (VSWR) were both significantly minimized.

In this paper, parasitic components with different geometries and designs are introduced into a near field WPT system (henceforth referred to as the PWPT system). Analyses are performed to investigate their effectiveness in enhancing the efficiency of the system. To obtain the optimum parameters for the designs, Simulated Annealing or SA optimization algorithm has been applied in conjunction with the method of moments (MoM) when computing the parameters.

In order to present a complete scheme, brief overview on the MoM and SA are first given in the subsequent sections. This is followed by a detailed elucidation on the design of the PWPT systems. Analyses based on the results obtained from the MoM and SA are discussed. A summary is then provided at the final section of the paper.

II. METHOD OF MOMENTS

The MoM is used to solve an E -field integral equation on the transmitting, receiving and loaded parasitic wire. The radius of the wire is assumed to be much smaller than the operating wavelength ($a \ll \lambda$) and the antenna length ($a \ll L$). The surface current on the wire is therefore axially directed, i.e., only the component flowing along the z -axis is considered.

The current J along the wire is approximated as the summation of piecewise sinusoidal expansion functions as:

$$J = \sum_{n=1}^M I_n J_n, \quad (1)$$

where J_n denotes the current on the n^{th} segment, M the number of expansion functions and I_n is the unknown coefficient to be obtained [4]. Then, the E -field integral equation on the wire is solved by the MoM and the following matrix equation is obtained:

$$[Z + Z_L][I] = [V], \quad (2)$$

where $[Z]$ is an $M \times M$ impedance matrix and the element Z_{ij} is the mutual impedance between the i th and j th segment. The $M \times M$ matrix $[Z_L]$ has only non-zero diagonal elements equal to impedance values at a receiving and a loading point [4]. Also, the unknown current $[I]$ and known feed voltage $[V]$ are an M -dimensional column vector. The element of $[V]$ corresponding to a feed point is only non-zero and is assumed 1 V. By solving (2), the antenna characteristics, including currents at the feed point I_t and receiving point I_r can then be obtained.

In this paper the efficiency is defined as:

$$e_f = \frac{P_r}{P_t} = \frac{\text{Re}(V_r I_r)}{\text{Re}(V_t I_t)}, \quad (3)$$

where $V_t = 1$ V at the feed point and,

$$V_r = -R_r I_r, \quad (4)$$

at the receiving point (R_r Ω is loaded). At the inductive load on the parasitic wire we have:

$$V_p = -jX_p I_p, \quad (5)$$

where jX_p is a loaded reactance on a parasitic wire. Load values R_r and jX_p in (4) and (5) are included in $[Z_L]$ in (2). The efficiency in (3) is then calculated by including the mutual coupling effects between all wires rigorously.

III. SIMULATED ANNEALING

The minimization search process in SA starts by generating an arbitrary initial point, x^0 . Based on the cost function C defined with respect to a scale proportional to the temperature T , the initial temperature TI and the temperature length TL are set. The function of TL is to determine the extent of search for the algorithm. The algorithm will then start by generating a random neighboring solution, x' . Once the two points – $C(x')$ and $C(x^{new})$ – are obtained, the cost function difference ΔC , which shows the difference between the existing point and the new point, can be determined by [5]:

$$\Delta C = C(x') - C(x^{new}). \quad (6)$$

If ΔC is greater than 0, that means the current point x^{new} is better than the initial point x' and x^{new} will overwrite x' . Otherwise, the program will generate a variable q , where the value of q will be randomly picked between 0 and 1. It then decides to accept or reject the inferior point. The decision to accept or reject the inferior point is based on the result obtained from the comparison between the calculated acceptance probability and the variable q . The calculated acceptance function A_p is given in (7) below:

$$A_p = \exp\left(\frac{\Delta C}{T}\right), \quad (7)$$

where T denotes the temperature. If the calculated value is near 1.0, then the new solution is taken to be better than its previous one. Otherwise, a value which is near 0 indicates that the new solution is worse. After each

iteration, the temperature T will decrease systematically according to the annealing schedule defined by the user. When T approaches zero, the probability the algorithm accepts a worse solution decreases correspondingly as well. The process will then repeat starting from generating a random neighboring solution until the algorithm reaches its termination condition, i.e., maximum number of iterations, computational time or maximum number of evaluations of the objective function.

IV. WIRELESS POWER TRANSMISSION

In this section, analyses on the performance of various WPT systems are performed. These include the conventional WPT (CWPT) system and the systems with parasitic elements installed into them (PWPT). Various designs of the PWPT system are proposed. The operating frequency used throughout the research work here is 1 GHz, voltage source at the transmitter V_s is 1 V and the load at the receiver R_L is 100 Ω .

A. Conventional WPT systems

In a CWPT system, energy is transferred via free space from an antenna connected to the source and it is then collected by the antenna at the receiving end [6]. A simplified schematic for the system is shown in Fig. 1. As can be observed from the figure, the transmitting antenna T_X is separated from the receiving antenna R_X by certain distance. The efficiency of wireless power transfer is determined when R_X is placed at different distance away from T_X . Here, center-fed half-wave dipoles are used for both antennas. The parameters used in the CWPT system are summarized in Table 1.

Figure 2 depicts the efficiency of the CWPT system, computed based on the MoM. As can be observed from the figure, the efficiency of the system decreases proportionately with distance as expected. This is to say that, the farther the receiver is placed away from the transmitting source, the more drastic the energy coupled to the antenna degrades. This has clearly restricted the distance for effective energy transmission in a CWPT system. Table 2 summarizes the peak efficiency and the effective distance of the CWPT system. Since the energy of the CWPT system deteriorates along with distance, the peak efficiency for wireless transmission is taken at the starting point where R_X is placed at distance 0.3λ away from the transmitter. For effective energy transmission, the minimum efficiency is set to be at 5%. This is to say that, the effective distance is taken at the position where the efficiency drops to 5%.

B. WPT systems with single parasitic wire

Figures 3 and 4 depict, respectively, the design configurations of the PWPT systems with a square and a circular parasitic wire installed into them. The distance between T_x and P_x is given as D_{P_x} and that between P_x and R_x is given as D_{R_x} . To give a fair comparison between

the two PWPT systems, the sizes of both parasitic wires are set to be identical.

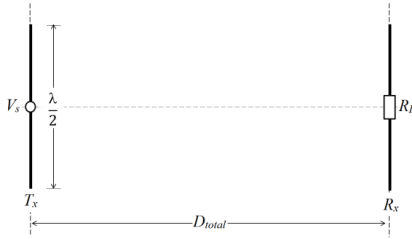


Fig. 1. A conventional WPT system, with half-wave dipole antennas.

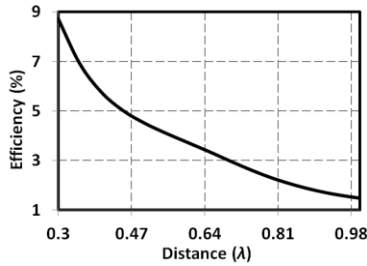


Fig. 2. Power efficiency of a conventional WPT system as a function of distance from the transmitter.

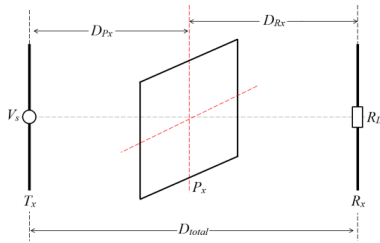


Fig. 3. A WPT system with a square parasitic wire.

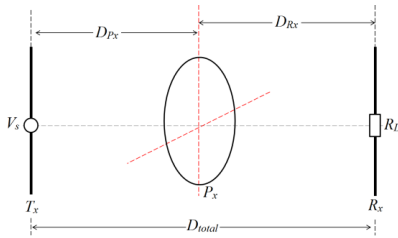


Fig. 4. A WPT system with a circular parasitic wire.

Table 1: Parameters of a CWPT system

Variables	Dimensions
T_x height (λ)	0.5
T_x radius (λ)	0.005
R_x height (λ)	0.5
R_x radius (λ)	0.01

Table 2: Performance of the CWPT system

Performance	CWPT
Peak efficiency (%)	8.72
Effective distance (λ)	0.45

In order to determine the optimum parameters for the design, the geometry, size, properties and position of the parasitic wires are taken as variables for optimization. Like the case of the CWPT system, the receiving antenna R_x is allowed to vary so as to compute the efficiency of the power coupled to it at varying distances from T_x . When performing optimization, P_x has been set to be either no impedance loading (i.e., both resistance R_p and reactance X_p are zero) or impedance loading (i.e., R_p and X_p are allowed to vary). The parameters for a square and circular parasitic wire P_x , obtained using SA are summarized in Table 3. Upon close inspection on the table, it can be observed that the resistance value R_p obtained using SA is 0Ω for optimum performance. Since resistance contributes to loss, it is therefore to be minimized in order to ensure efficient energy coupling. Reactance loading is one of the methods to improve antenna characteristics [4] and it is interesting to introduce it to optimize near-field power efficiency.

Figures 5 to 8 depict the power efficiency of the reactive WPT systems in terms of distance λ . The curves in the figures show that the system obtained its peak efficiencies at about 0.37λ using a square and circular P_x . The peak efficiency is some distance away from the transmitter because the receiver antenna may collect additional energy scattered from the parasitic wire in addition to the reception of direct electromagnetic energy from the transmitter [7]. The curves in the figures show that the system gives the highest power efficiency with the presence of an inductive P_x . Table 4 summarizes the peak efficiencies and effective distances found in Figs. 5 to 8. As shown in the table, the peak power efficiency when a reactive component is included in P_x is about 0.79% (for the square geometry) to 1.0% (for the circular geometry) higher than that of the zero-impedance case. It can also be seen that a square reactive P_x performs better than its circular counterpart. The peak efficiency attained using the square P_x is 0.69% higher than the circular P_x . When the receiver moves farther away from the transmitter, the power coupled to the receiver antenna tends to decrease. Hence, the power efficiency decreases accordingly as well. As depicted in Figs. 7 and 8, at a distance of 0.5λ to 1λ , the efficiencies using the square and circular P_x are comparable. By comparing Tables 2 and 4, it can be seen that the peak efficiency of the inductive square PWPT system is about 5.82% higher than that of the CWPT system. The effective distance of the square P_x is also approximately 0.32λ farther than that of the CWPT system.

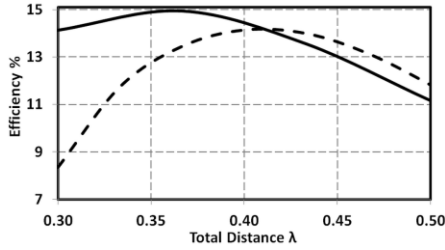


Fig. 5. Performance of WPT systems with zero-impedance (dashed line) and inductive (solid line) square parasitic wires, at distance 0.3λ to 0.5λ .

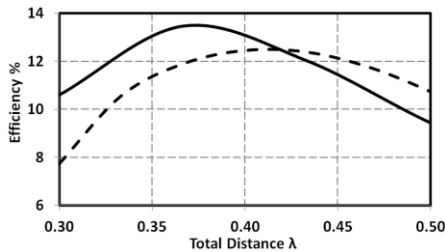


Fig. 6. Performance of WPT systems with zero-impedance (dashed line) and inductive (solid line) circular parasitic wires, at distance 0.3λ to 0.5λ .

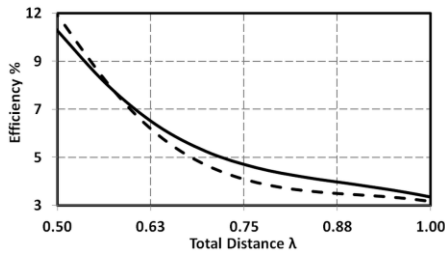


Fig. 7. Performance of WPT systems with zero-impedance (dashed line) and inductive (solid line) square parasitic wires, at distance 0.5λ to 1.0λ .

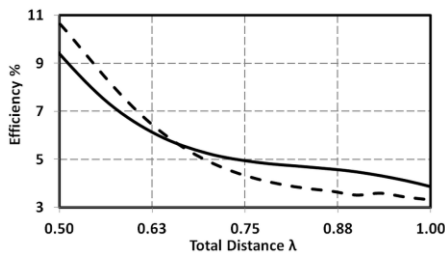


Fig. 8. Performance of WPT systems with zero-impedance (dashed line) and inductive (solid line) circular parasitic wires, at distance 0.5λ to 1.0λ .

In order to obtain a better insight on the effect of inductance in parasitic wires, the current generated at each part of the system is investigated. Figure 9 illustrates the points and expansion functions set up in

the MoM to calculate the current in the square PWPT system. It is clear from the figure that each point and expansion function corresponds to different parts of the system. The impedances Z_p are placed at expansion function $n = 21$ and 33 . It is to be noted that Z_p is a complex variable which consists of $R_p = 0 \Omega$ and $X_p = 17.26 \Omega$, i.e., $Z_p = 0 + j17.26 \Omega$.

Figures 10 to 12 depict the current distribution at the transmitter, receiver and parasitic wire when the receiver is 0.5λ away from the transmitter. According to the curves shown in Fig. 7, the efficiency of the power coupled to the receiver is about 10.76% when $D_{RX} = 0.5\lambda$. Due to the effect of the parasitic element the real part of I_t has a peak and the imaginary part of I_t has a notch to reduce the imaginary power which stores the energy. Then real power P_t is transferred efficiently to the receive antenna. Therefore the current at the feed has a notch as shown in Fig. 10. At the receive antenna the larger receive power is transferred and the current amplitude has a peak as shown in Fig. 11.

Table 3: Parameters of a PWPT system

Variables	Square P_X	Circular P_X
P_X length (λ)	1.0	1.00
P_X radius (λ)	0.005	0.005
D_{PX} (λ)	0.161	0.154
D_{RX} (λ)	0.189	0.209
R_p (λ)	0.00	0.00
X_p (λ)	17.26	13.27

Table 4: Performance of a PWPT system

Configuration	Peak Efficiency (%)	Effective Distance (λ)
Lossless square geometry ($R_p = X_p = 0$)	13.75	0.70
Inductive square geometry ($R_p = 0, X_p = 17.26 \Omega$)	14.54	0.77
Lossless circular geometry ($R_p = X_p = 0$)	12.85	0.70
Inductive circular geometry ($R_p = 0, X_p = 13.27 \Omega$)	13.85	0.77

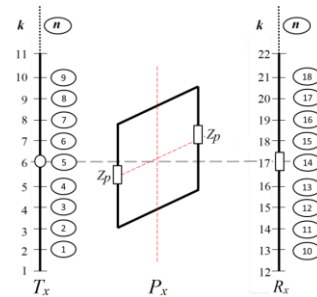


Fig. 9. Points (k) and expansion function (n) numbering of the PWPT system.

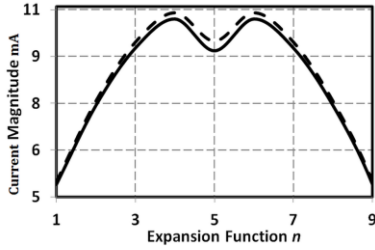


Fig. 10. Current distributions at the transmitter of a WPT system with an inductive (solid line) and zero-impedance (dashed line) parasitic wire.

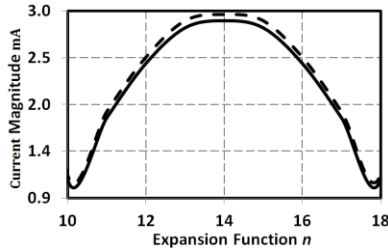


Fig. 11. Current distributions at the receiver of a WPT system with an inductive (solid line) and zero-impedance (dashed line) parasitic wire.

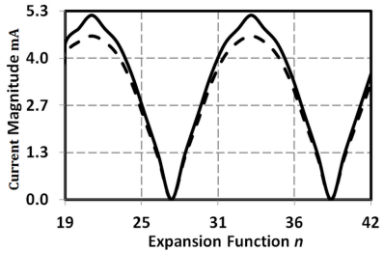


Fig. 12. Current distributions at the parasitic wire of a WPT system with an inductive (solid line) and a zero-impedance (dashed line) parasitic wire.

It can be seen from Fig. 12 that the current distributions produced at expansion functions ranging from $n = 19$ to 24 and 31 to 36 are higher than those at $n = 25$ to 30 and 37 to 42 . The former two ranges of expansion functions correspond to the left and right parts of the wire which are in parallel with the antennas and the wave polarization; whereas, the latter two correspond to the top and bottom parts which are in orthogonal. The result indicates that higher current is produced at the wire when it is parallel to the direction of the wave polarization. With proper orientation, it can be seen that the wire in parallel with the direction of wave polarization is longer for a square wire compared to a circular one. Hence, the system with a square P_x exhibiting better performance than that with a circular P_x is to be expected. Figure 12

also shows that the current distributions found at the inductive wire are higher than those parts with zero impedance. Indeed, the current peaks at $n = 21$ and 33 , i.e., the positions where both inductances are placed. It is therefore evident that the presence of inductance (which is an energy storage device) helps to enhance the current produced at the parasitic wire.

C. WPT systems with dual parasitic wires

Based on the results obtained in the previous section, it can be concluded that a PWPT system enhances both the peak efficiency and the effective distance of wireless power transmission and that a square (rather than a circular) P_x is a better option for the system. In this section, an additional square P_x is therefore proposed to be integrated into the system to study its impact on performance enhancement.

Figure 13 shows the configuration of a PWPT system with dual parasitic wires (henceforth referred to as the PPWPT system). Two parasitic wires P_{x1} and P_{x2} are placed along the same axis with the transmitting antenna T_x sandwiched in between both. The distance between P_{x1} and T_x is denoted as D_{Px1} and that between P_{x2} and T_x as D_{Px2} . Similarly, the distance between the receiving antenna and P_{x1} is denoted as D_{Rx} . The optimum parameters for an inductive system are tabulated in Table 5. The performance of the system with respect to the total distance D_{total} from R_x to P_{x2} is shown in Fig. 14. The peak efficiency and effective distance of the system are summarized in Table 6. It is apparent from the table that the effective distance of the system is found to have extended close to 1λ . This is to say that, the distance it takes for the efficiency of the system with dual P_x to drop below 5% is relatively longer than that with a single P_x . By comparing Tables 4 and 6, it can also be seen that the magnitude of the peak efficiencies and effective distances are about 3.37% higher and 0.18λ farther than those with a single P_x . Hence, it can be concluded here that the performance of the WPT system can be significantly improved when the number of parasitic wires increases. This is particularly so, when the wires are placed at the front and back of the transmitting antenna.

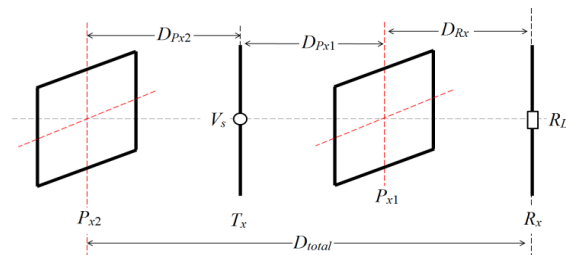


Fig. 13. A PPWPT system.

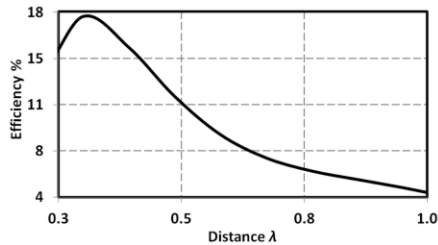


Fig. 14. Performance of a PPWPT system.

Table 5: Parameters of a PPWPT system

Variables	Dimensions
P_X length (λ)	1.0
P_X radius (λ)	0.005
D_{PX1} (λ)	0.173
D_{PX2} (λ)	0.30
D_{RX} (λ)	0.173
R_P (Ω)	0
X_P (Ω)	19.33

Table 6: Performance of a PPWPT system

Performance	Inductive Square PWPT
Peak efficiency (%)	17.91
Effective distance (λ)	0.95

V. CONCLUSION

In this paper, the optimization procedure of wireless power transmission systems with parasitic wires is presented in detail. By implementing the MoM in conjunction with SA, the geometry, size, properties and position of the parasitic wires are optimized. When a square inductive wire is integrated in between the transmitter and receiver, the result gives the highest peak power efficiency and longest effective distance for power coupling. The performance of the system can be further enhanced when an additional square wire is placed at the back of the transmitter.

REFERENCES

- [1] X. Jin, J. M. Caicedo, and M. Ali, "Near-field wireless power transfer to embedded smart sensor antennas in concrete," *ACES J.*, vol. 30, no. 3, pp. 261-269, 2015.
- [2] A. Kurs, A. Karalis, R. Moffatt, J. D. Joannopoulos, P. Fisher, and M. Soljacic, "Wireless power transfer via strongly coupled magnetic resonances," *Science Express*, vol. 317, no. 5834, pp. 83-86, 2007.
- [3] M. D. Migliore, D. Pinchera, and F. Schettino, "A simple and robust adaptive parasitic antenna," *IEEE Transactions on Antennas and Propagation*, vol. 53, no. 10, pp. 3262-3272, 2005.
- [4] K. Hirasawa and M. Haneishi, *Analysis, Design and Measurement of Small and Low-Profile Antennas*. 1st ed., Boston, USA, Artech House,

1992.

- [5] D. Bertsimas and J. Tsitsiklis, "Simulated annealing," *Statistical Science*, vol. 8, no. 1, pp. 10-15, 1993.
- [6] A. R. C. Cheah, K. H. Yeap, K. C. Yeong, and K. Hirasawa, "Biologically inspired wireless power transmission system: A review," In: V. Ponnusamy, N. Zaman, T. J. Low, and A. H. M. Amin, *Biologically-Inspired Energy Harvesting Through Wireless Sensor Technologies*. 1st ed., Hershey PA, USA, IGI Global, pp. 27-50, 2016.
- [7] A. R. C. Cheah, K. H. Yeap, K. Hirasawa, K. C. Yeong, and H. Nisar, "Optimization of a wireless power transmission system", in Proc. of the Int. MultiConference of Engineers and Computer Scientists; Hong Kong, pp. 590-592, 2016.



Kim Ho Yeap received his Ph.D. from Universiti Tunku Abdul Rahman. He is currently an Associate Professor in Universiti Tunku Abdul Rahman.



Agnes Ruey Chyi Cheah received her B. Eng. (Hons) Electronics Engineering at Tunku Abdul Rahman University. She is currently pursuing her Master degree in the same university.



Kazuhiro Hirasawa received his Ph.D. from Syracuse University, USA in 1971. He is currently an Emeritus Professor in University of Tsukuba, Tsukuba, Japan. His research interests include wireless power transmission.



Kee Choon Yeong received his Ph.D. from Rensselaer Polytechnic Institute. He is currently an Assoc. Professor in Universiti Tunku Abdul Rahman.



Koon Chun Lai received his Ph.D. from Universiti Tunku Abdul Rahman. He is currently an Assistant Professor in Universiti Tunku Abdul Rahman.



Humaira Nisar received her Ph.D. from Gwangju Institute of Science and Technology. She is currently an Associate Professor at Universiti Tunku Abdul Rahman.